Available online at www.sciencedirect.com
SCIENCE DIRECT®
PERGAMON
International Journal of Heat and Mass Transfer 46 (2003) 2445–2457
International Journal of HEAT and MASS TRANSFER
www.elsevier.com/locate/ijhmt

Online fouling detection in electrical circulation heaters using neural networks

Sylvain Lalot [a,b,*], Stéphane Lecoeuche [a,c]

[a] M.E.T.I.E.R., E.I.P.C., Campus de la Malassise, BP 39, 62967 Longuenesse Cedex, France
[b] LME, Université de Valenciennes, Le Mont Houy, BP 311, 59304 Valenciennes Cedex, France
[c] Laboratoire I3D, Bâtiment P2, Université de Lille 1, 59655 Villeneuve d'Ascq Cedex, France

Received 23 January 2002; received in revised form 19 October 2002

Abstract

Here is presented a method that is able to detect fouling during the service of a circulation electrical heater. The neural based technique is divided in two major steps: identification and classification. Each step uses a neural network, the connection weights of the first one being the inputs of the second network. Each step is detailed and the main characteristics and abilities of the two neural networks are given. It is shown that the method is able to discriminate fouling from viscosity modification that would lead to the same type of effect on the total heat transfer coefficient.

1. Introduction

Circulation electrical heaters are widely used in many processes [1–4]. To reduce the response time of some heaters, it is possible to generate the Joule effect in the tube wall. In that case the temperature difference between the product to be heated and the heater is small. This property is used to sterilize milk without giving it a disagreeable taste. It is also used when high temperatures are required. For example, the air that is needed in blast furnaces can be heated to about 1,400 K to increase the efficiency of the chemical reactions. The small temperature difference between the air and the tubes reduces the risk of creeping for the heating tubes. In all cases it is necessary to have an accurate model of the heater to make the control very efficient [5]. But in many cases fouling may occur in the heater. As it is well known that this could be harmful [6,7], different approaches are developed to tackle the problem of fouling. The first one tries to avoid fouling using electronic devices [8–10], the second one tries to avoid fouling using adequate geometries [11] or surface treatment [12,13]. The last approach is to try to detect fouling itself. The classical approach for fouling detection is to measure the thermal resistance [14]. In this case it is necessary to introduce temperature sensors in the studied system. An ultrasonic technique has also been tested [15]. For these last two methods, only few points could be monitored in practice. Non-intrusive methods are developed such as a recirculation loop used by Asomaning and Watkinson [16]. It is also possible to use models for fouling, e.g. [17], and to use these models in heat exchangers computation [18,19].

This shows that there is a need for a global monitoring system. In a first step towards this goal, the aim of the present study is to show the feasibility of the detection of fouling in an electrical circulation heater using the actual service data (obtained by simulation for this study).

As neural based techniques have proved to be efficient in identification of thermal systems [20–25], in identification of large systems [26], in estimation or modeling of fouling in some chemical processes [27,28] and in drifts detection [29,30], it has been chosen here to develop such a technique for online fouling detection.

First, the governing equations of transient states are presented. It is shown that only two dimensionless

* Corresponding author. Address: M.E.T.I.E.R., E.I.P.C., Campus de la Malassise, BP 39, 62967 Longuenesse Cedex, France. Tel.: +33-3-21-38-85-10; fax: +33-3-21-38-85-05.
E-mail addresses: slalot@eipc.fr (S. Lalot), slecoeuche@eipc.fr (S. Lecoeuche).

0017-9310/03/$ - see front matter
doi:10.1016/S0017-9310(02)00545-8

Nomenclature

A	heat exchange area (m^2)
C_i	class #i detected by the classifier
c	specific heat (J/kg K)
$D(P_j, I)$	distance between prototype P_j and input vector I (classifier)
e_c	thickness of fouling (m)
I	input vector (classifier)
L	length of the heater (m)
n_o	number of regressors for the output (first network)
n_{i1}	number of regressors for the first input (first network)
n_{i2}	number of regressors for the second input (first network)
n_c	number of neurons in the classifier output layer
n_p	number of neurons in the classifier hidden layer
n_w	number of neurons in the classifier input layer
P_j	prototype of the classifier
Q_v	volumic heat source (W/m^3)
R	dimensionless parameter
r_1	inner tube radius (m)
S	dimensionless parameter
T	temperature (K)
t	time (s)
t^+	dimensionless time
V	volume per unit length (m^3/m)
w	fluid velocity (m/s)
x	abscissa (m)
x^+	dimensionless abscissa

Greek symbols

α	heat transfer coefficient (W/m^2 K)
θ	dimensionless temperature
φ	regression vector
λ	thermal conductivity (W/m K)
μ	activation function (classifier)
Ψ	membership degree of a prototype to a class (classifier)
ρ	density (kg/m^3)
σ	size of the influence of a prototype (classifier)

Subscripts

c	clogging (fouling)
f	fluid
i	inlet or input
nom	nominal
o	outlet or output
t	tube

parameters are required to fully characterize a circulation electrical heater. It is also shown that to be able to detect fouling, it is necessary that the model takes into account simultaneous variations of the mass flow rate and of the heat rate. Then the principles of online drifts detection using coupled neural networks are presented. The analysis is then divided in two major steps: the first step is "online identification", the second step is "surveying and classification". In the first step, identification is studied through the influence of the size of the identification window. In the second step, the connection weights of the first network are determined for 17 configurations (normal functioning, four fouling stages, four fluid characteristics modifications, eight fouling and fluid characteristics modifications). Then the classifier, that is based on pattern recognition techniques, is introduced. The inputs of this classifier are the connection weights of the first network. Its main abilities are: unsupervised learning and self-adaptation of its architecture; this second network is able to create, on its output layer, new neurons that characterize new kinds of deviations. This ability is used to discriminate the different sets of connection weights that are obtained for fouling and fluid characteristics modifications.

2. Governing equations

Circulation electrical heaters in which the heat is created by the Joule effect in the tube walls are usually a combination of several tubes. These tubes are coupled in such a way that they are in parallel for the flow (and in any arrangement for electricity). So, it is only necessary to study the behavior of a single tube. A schematic of the tube is shown in Fig. 1.

In general, the thermal resistance between the fluid and the tube is much higher than the thermal resistance of the tube itself. So, it is possible to assume that the variation of the temperature is negligible along the ra-

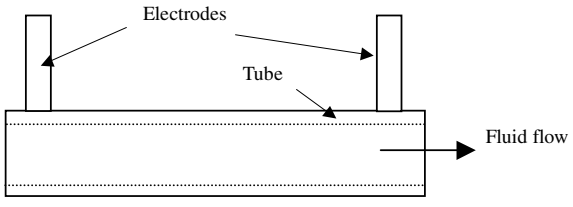

Fig. 1. Schematic of the studied circulation electrical heater.

dius in the tube wall. Likewise, conduction in the axial direction of tube is assumed to be negligible as is done in the study of heat exchangers [31]. The fluid temperature is supposed to be uniform in a cross-section of the tube; so, it depends only on the distance to the inlet. The tube is supposed to be well insulated. So, the heat losses to the ambient air are neglected. Under these assumptions, two energy balances can be written; the first one (Eq. (1)) for the tube; the second one (Eq. (2)) for the fluid.

$$\frac{\alpha A}{L}(T_t - T_f)\,dx + V_t\rho_t c_t \frac{\partial T_t}{\partial t} = Q_v V_t\,dx \tag{1}$$

$$\frac{\alpha A}{L}(T_t - T_f)\,dx = V_f\rho_f c_f\left[\frac{\partial T_f}{\partial t} + w\frac{\partial T_f}{\partial x}\right]dx \tag{2}$$

The heat transfer coefficient is computed as follows:

$$\frac{1}{\alpha A} = \frac{1}{\alpha_c 2\pi(r_1 - e_c)L} + \frac{1}{2\pi\lambda_c L}\ln\left(\frac{r_1}{r_1 - e_c}\right) \tag{3}$$

where α_c is computed using the following correlation: $Nu = 0.023Re^{0.8}Pr^{1/3}$.

Extracting T_t from Eq. (2) and introducing it in Eq. (1), leads to the governing equation (Eq. (4)).

$$[V_f\rho_f c_f + V_t\rho_t c_t]\frac{\partial T_f}{\partial t} + wV_f\rho_f c_f\frac{\partial T_f}{\partial x} + V_t\rho_t c_t\frac{L}{\alpha A}V_f\rho_f c_f\frac{\partial^2 T_f}{\partial t^2} + V_t\rho_t c_t\frac{L}{\alpha A}V_f\rho_f c_f w\frac{\partial^2 T_f}{\partial x\,\partial t} = Q_v V_t \tag{4}$$

To make Eq. (4) dimensionless, the following reduced variables can be introduced:

$$x^+ = \frac{x}{L},\quad t^+ = \frac{t}{L/w}$$

$$\text{and}\quad \theta = \frac{T_f(x,t) - T_{fi}}{T_f(L,+\infty) - T_{fi}},$$

$$\text{with}\quad T_f(L,+\infty) = \frac{Q_v V_t L}{w_{nom}V_f\rho_f c_f} + T_{fi}.$$

Then two dimensionless parameters appear: $R = (V_t\rho_t c_t)/(V_f\rho_f c_f)$ and $S = (V_t\rho_t c_t w)/(\alpha A)$.

Note that the ratio R/S is the number of transfer units (N_{tu}) of the traditional heat exchangers.

Finally, it is possible to write the desired equation (Eq. (5)).

$$(1+R)\frac{\partial\theta}{\partial t^+} + \frac{\partial\theta}{\partial x^+} + S\frac{\partial^2\theta}{\partial t^{+2}} + S\frac{\partial^2\theta}{\partial x^+\partial t^+} = 1 \tag{5}$$

It is important to note that the dimensionless temperature, based on the nominal velocity, might be greater than unity. It is also important to note that, in the studied case, it has been considered that the mass of the fouling material is much lower than the mass of the tube and of the fluid. Hence, parameter R is considered as constant.

On the contrary, parameter S varies with the mass flow rate through the fluid velocity itself w and through the heat transfer coefficient α. The variations of parameter S through the heat transfer coefficient could have many origins according to Eq. (3), e.g. the variation of the fluid viscosity or the variation of the fouling thickness.

To discriminate the influence on parameter S of the variations of the mass flow rate from the influence of fouling or viscosity modification, the model that detects drifts should be independent of the mass flow rate (the variation of α with the mass flow rate is then already taken into account). Hence, it is necessary to get a multiple inputs single output (MISO) model. In our case, the inputs are the mass flow rate and the heat rate, and the output is the outlet fluid temperature. To show that fouling influences the behavior of an electrical circulation heater, it is informative to plot (Fig. 2) the responses of a heater with and without fouling for the same solicitations (mass flow rates and heat rates). The solutions are computed using a finite difference scheme.

It is also important to note that the present study is based on the numerical resolution of Eq. (5). So, the inputs of the neural network would have been "clean" data. In practice, noise would be present in the data and the identification technique should be noise-insensitive. It can be shown that neural based techniques have this ability as far as the noise is not correlated with the input. Considering an arbitrary second order system, considering a random input sequence, an output sequence is obtained. A first neural network is trained using this couple of data. Then, noise is added to the output sequence: random noise that is proportional (20%) to the mean value of the outputs, combined with a random noise that is proportional (20%) of the instantaneous output. A second network is trained using the input sequence and the new noisy output sequence. Finally, considering a new random input sequence, the output sequences of both networks are compared. Fig. 3 shows, on the left-hand side, the output sequences that are

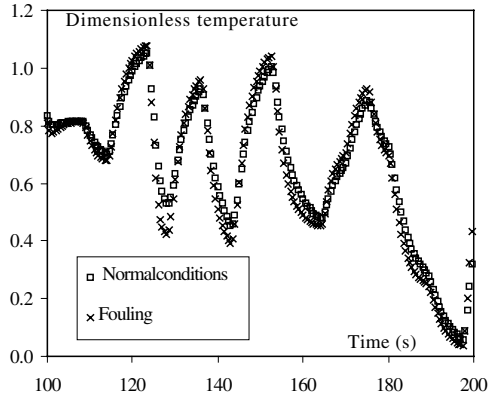

Fig. 2. Responses of a heater with and without fouling.

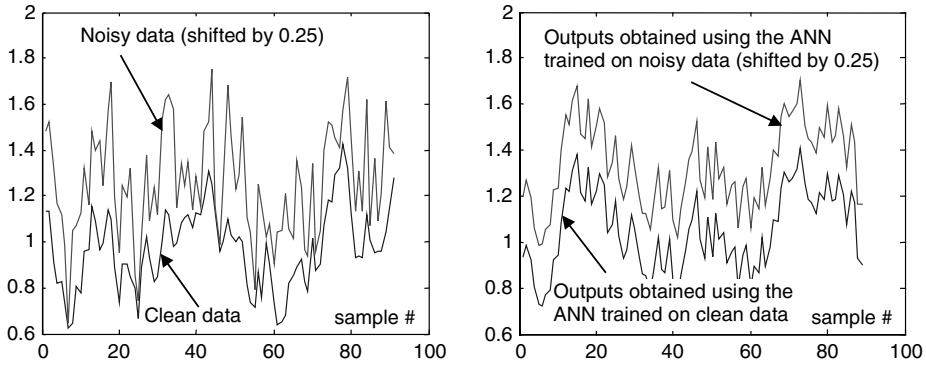

Fig. 3. Illustration of the insensibility of the neural based identification technique.

taken into account for the training of the networks and on right-hand side the outputs that are obtained when considering the second input sequence. The RMS error being less than 0.5% of the mean value of the clean data, it can be concluded that the neural based technique is actually noise-insensible.

3. Principles of drifts detection

The detection technique is based on coupling online identification with connection weights surveying as described now. Fig. 4 shows a schematic of the supervision system that is used in the present study.

The system consists of two neural networks. The first neural network is based on the principles of non-linear online identification. Using the past input and past output data stemmed from the system, the neural network adapts its architecture (adapts the weights between the different neurons) in order to model the system to be surveyed. Generally, for MISO systems, the output is made of one neuron that is the present estimated output. Identification is always made during the service of the system. So, the connection weights are representative characteristics of the model of the system in its current state. As it is possible to consider the architecture of this first network as an accurate black-box model of the actual system, it is possible to detect any deviation of the real system by surveying the evolution of the neural architecture.

The second network is based on pattern recognition techniques. Its aim is to detect the evolution of the model and recognize the cause of the deviation. The inputs of this classifier are the connection weights of the first network. This classifier is characterized by its main abilities: unsupervised learning and self-adaptation of its architecture. It is able to create, on its output layer, new neurons that would characterize new kinds of deviations.

4. Online identification

The neural based online identification has been presented in [32–36]. Fig. 5 summarizes the identification process:

Each step of the identification process is detailed below for the identification of the circulation electrical

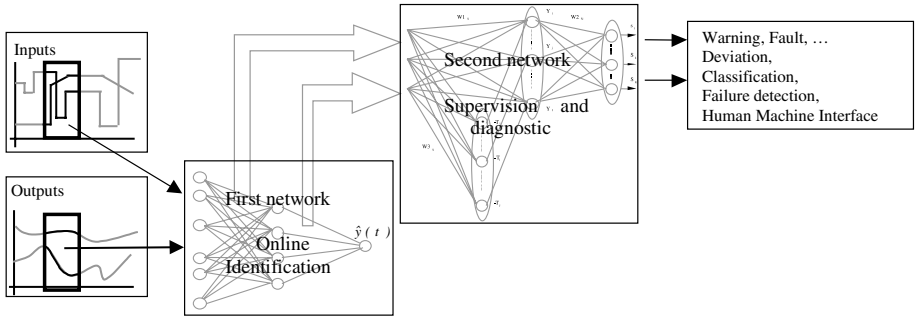

Fig. 4. Architecture of the drifts detection system.

heater. This identification is carried out when the heat rate is randomly changed at random times. Fig. 8 gives an example of the response.

4.1. Description of the studied heater

The present study is based on an actual 10 kW water heater. This heater is made of stainless steel and has the following characteristics:

Tube		Fluid	
Inside Ø	14 mm	Nominal velocity	0.8 m/s
Outside Ø	16 mm	Inlet temperature	20 °C
Length	1 m	Heat transfer coefficient	Colburn correlation

This leads to the following values for R and S (for nominal velocity): $R = 0.27$, $S = 1.5$. In order to get significant temperature variations, the following ranges have been chosen:

$0\% <$ heat rate (input #1) $< 100\%$,

0.6 m/s $<$ velocity (input #2) < 1 m/s,

2 s $<$ random duration for stages < 10 s.

In this case the mean value of the duration of the stages is 6 s.

4.2. Determination of the structure of the model

According to previous works [37,38], the neural network output error (NNOE) model is tested (cf. [35] for details on this architecture). The structure that is looked for is the simplest one that gives accurate results; a classical three layers network. The influence of the number of neurons in the hidden layer is studied along with the influence of the composition of the regression vector $[n_0 \quad n_{i1} \quad n_{i2}]$ = [number of considered outputs, number of considered inputs #1, number of considered inputs #2].

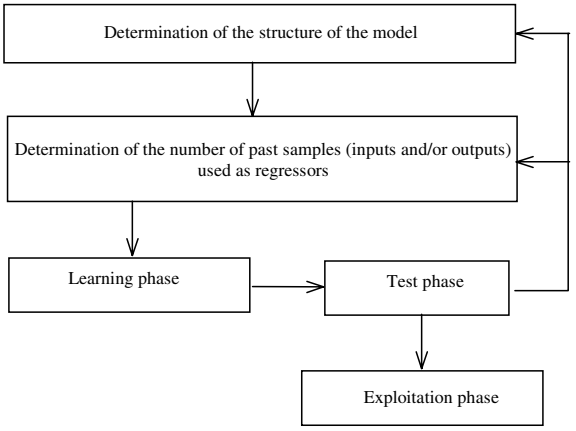

Fig. 5. Schematic of the identification process.

Table 1
Evolution of the distance between the models and the real system versus the number of neurons

Number of neurons in the hidden layer	Composition of the regression vector $[n_o \quad n_{i1} \quad n_{i2}]$	Distance
1	[2 2 2]	1 (reference)
	[3 3 3]	1.0013
	[5 5 5]	1.0002
	[10 10 10]	0.9999
2	[2 2 2]	1
	[3 3 3]	1.0013
	[5 5 5]	1.0002
	[10 10 10]	0.9999
3	[2 2 2]	1
	[3 3 3]	1.0013
	[5 5 5]	1.0002
	[10 10 10]	0.9999

Once the model is chosen, it is necessary to determine the number of neurons in the hidden layer. Table 1 shows the values of the relative Euclidean distance between the models and the real system for three numbers of neurons in the hidden layer.

It can be seen that the values of the distance are independent of the number of neurons in the hidden layer. It can be concluded that a unique neuron in the hidden layer is sufficient.

4.3. Determination of the composition of the regression vector

Fig. 6 shows the typical evolution of the distance between the estimated and known outputs versus the composition of the regression vector; in all cases the number of past estimated outputs, of past heat rates and past mass flow rates are equal (1, 2, 3, 5, 10).

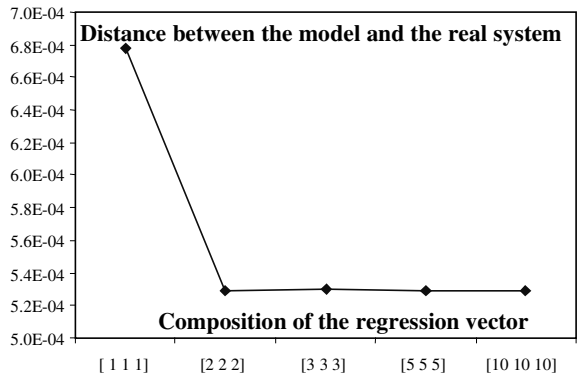

Fig. 6. Distance between the model and the real system versus the composition of the regression vector.

It can be concluded that a regression vector built using two past estimated outputs, two past heat rates and two past mass flow rates is sufficient, no significant improvement being noticed using larger regression vectors. It is interesting to remind that, on the one hand, it has been shown [39] that circulation electrical heaters can be considered as second order systems when responding to fluid flow variations, and on the other hand, it has also been shown that they can be considered as second order systems when responding to heat rate variations [23].

4.4. Learning and test phases

It is during these phases that the size of the observation window (Fig. 7) has to be determined. The width of the identification window is considered as a parameter that has to be optimized for a fixed offset. It has been chosen here to fix the offset to the width of the window.

As can be seen the whole learning database is 6000 s long. This corresponds to thousand times the mean value of the duration of the stages. The width of the identification window varies from 30 to 120 s (i.e. 5–20 times the mean duration of the stages).

Fig. 8 shows the evolution of the mean value of weight #1 versus the number of identifications and the histogram of instantaneous values of this weight. Note that the mean value for identification #*n* takes into account the values of the weight from the first identification to the *n*th identification.

It can be seen that convergence is not obtained for 30 s. It can also be seen that the wider the identification

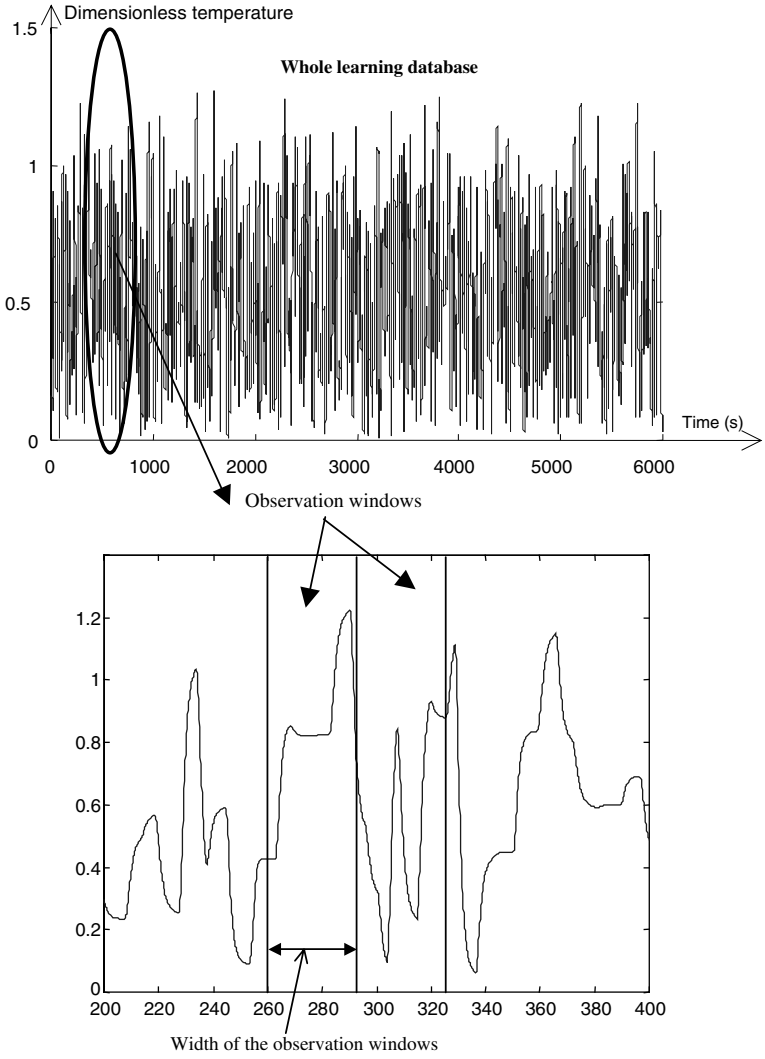

Fig. 7. Definition of the width of the observation windows.

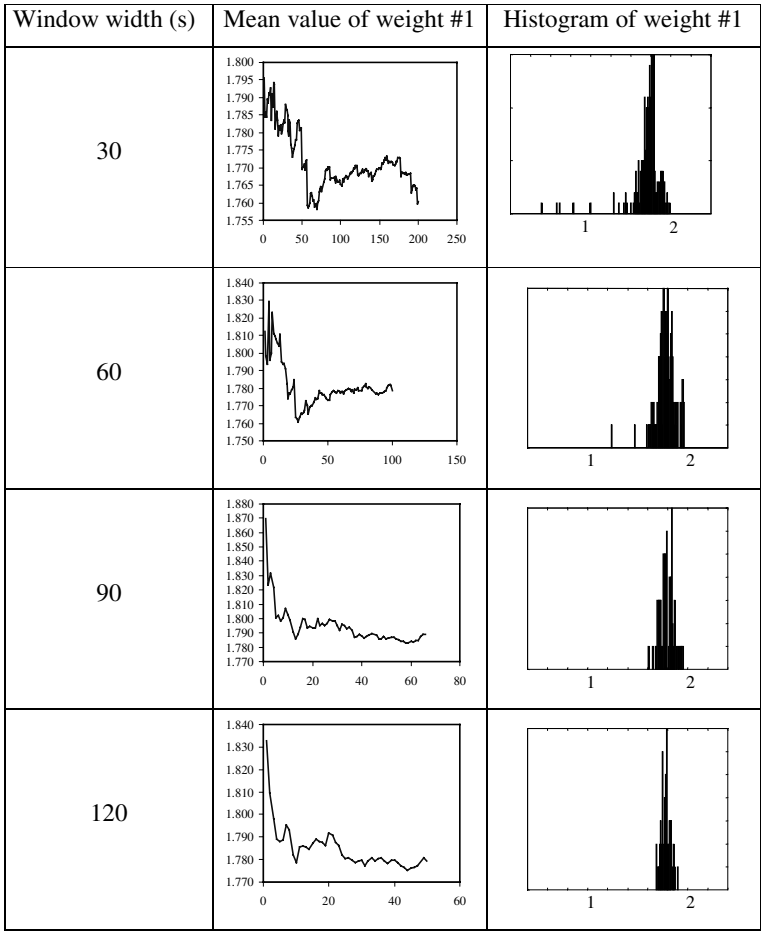

Fig. 8. Evolution of the mean value and of the histogram of weight #1 for various window widths.

window, the thinner the histogram but the longer the computational time (for a constant sample period = 1 s). So, to choose the identification window width, it is interesting to look at the final value of the weights. Table 2 shows the final values of the first two weights depending on the window width.

It can be seen that whatever the window width is (but larger than 10 times the mean duration of the stages), an accurate value of the weight is obtained (the differential between a weight and the mean value of this weight is less than 1%). To make a compromise between the quality of the histogram and the computational time, a window width of 90 s (15 times the mean stage duration) is chosen. For this value, it is possible to show that all weights have converged (Fig. 9). The analysis of the histograms shows that the results are accurate.

Table 2
Final values of weight #1 and #2 versus the width of the identification window

	Window width		
	60 s	90 s	120 s
Weight #1	1.77873	1.78888	1.77925
Weight #2	−0.78905	−0.79890	−0.78980

Now that the width of the identification window is determined, it is possible to go on with the exploitation phase.

4.5. Exploitation phase

The exploitation phase is the final goal of the identification step. In this study, arbitrary fouling has been introduced in the model. Its thickness varies from 0 to 2 mm in four evenly spaced steps, and its thermal properties are those of calcium.

For fouling detection, it is necessary to know the values of all weights for each fouling stage (Fig. 10).

To know if these values actually characterize fouling, it is interesting to compare them with the values of the weights when the variations of the equivalent heat

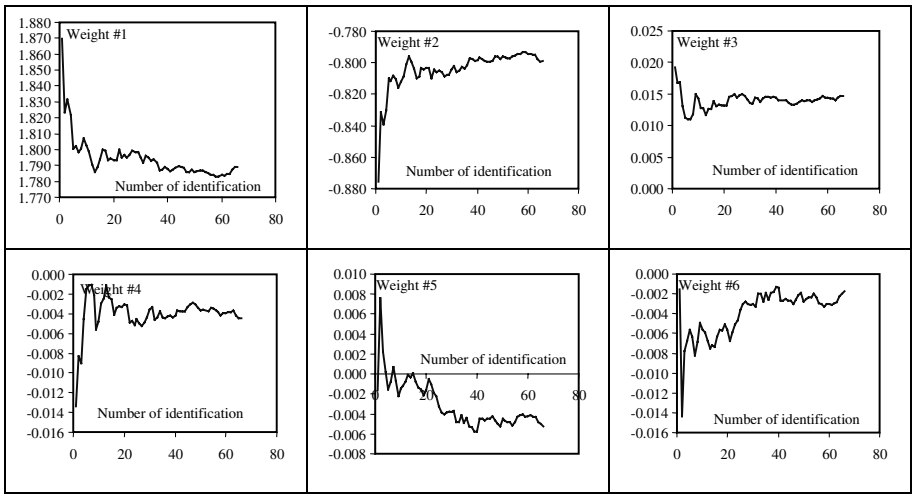

Fig. 9. Convergence of all weights.

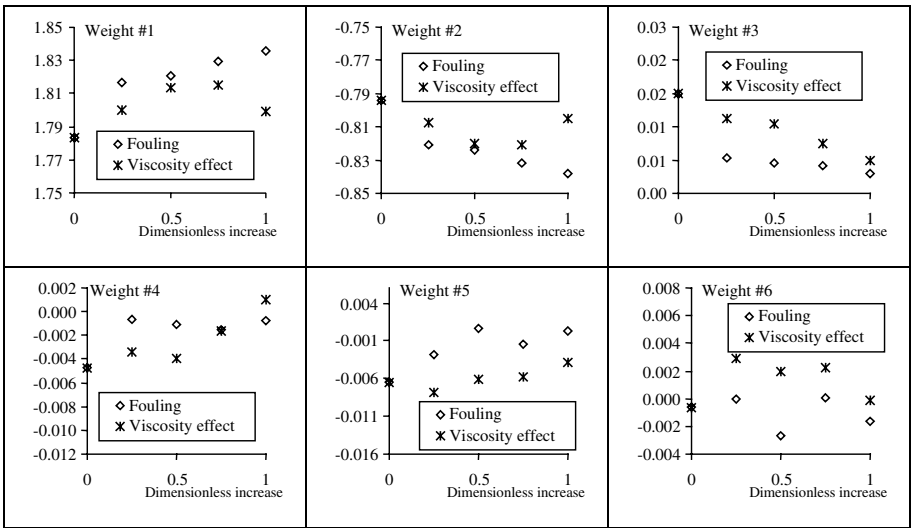

Fig. 10. Compared effects of viscosity and fouling on the weights.

transfer coefficient is caused by another phenomenon. It has been chosen here to act on the viscosity of the fluid. The higher the viscosity, the lower the heat transfer coefficient. Fig. 11 shows that the effect of viscosity is similar to the effect of fouling.

Even though the effects are similar, the values of the weights are different; Fig. 12 shows the values of the weights in both cases. The maximum viscosity ratio has been fixed to 4 (this corresponds [40] to a temperature change of 20° for oil at about 310 K, of less than 30° for glycerin at 310 K), and the maximum fouling thickness is kept to 2 mm.

The dimensionless increase is the ratio of the present increase to the maximum increase (in four steps) taken into account for the parameters. The combination of fouling and viscosity increase leads to other sets of values as shown in Fig. 14, where step 0 represents the normal conditions and each step corresponds to a step of viscosity (increasing viscosity) and a step of fouling (increasing thickness).

The last set of connection weights is determined when the viscosity decreases and when fouling occurs (Fig. 13).

The role of the second network is to analyze the data that have been obtained during the online identification. It has to answer the question: ''Are all the combinations of the connection weights different?''. In practice, other drifts could appear (others sets of connection weights

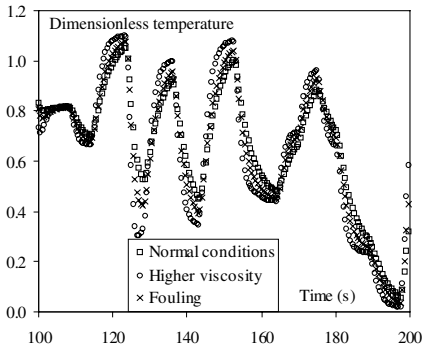

Fig. 11. Compared effects of viscosity and fouling on time response.

would appear), the evolutions would be continuous. So, it should be necessary to use a auto-adaptive classifier.

In the present study, such a powerful classifier is used to show the feasibility of online fouling detection. In a first step, during an unsupervised phase, it is shown that the classifier is able to detect the 16 sets of connection weights that correspond to the 16 drifts. It is important here to remind that it is not an obviousness that fouling and viscosity change (that have similar effects on the outlet fluid temperature) correspond to different sets of connection weights. In a second step, the classifier is "frozen" and is used as a "normal" (non-adaptive) classifier.

5. Principles of unsupervised classification

Generally speaking, classification aims at grouping similar objects into classes. Two cases are conceivable. In the first case, the number of classes to be created is a priori known; a classical classifier is efficient. In the second case, the number of classes is a priori not known; the classifier should be able to create new classes corresponding to totally new objects. This leads to choose a classifier which has unsupervised learning abilities and which is also able to create new prototypes.

In our case, the objects are the connection weight vectors coming from the first network and the classes are the types of deviations that are studied. For example, normal fluid (nominal viscosity) flowing in a clean circulation heater makes one class (small variations are possible around the nominal functioning point); normal fluid flowing in a heater in which fouling occurs makes a second class; high viscosity for the fluid flowing in a clean heater makes a third class, and so on. Hence, it has to be considered that the number of classes is a priori not known. This is why the study focuses on classifiers which have special abilities (unsupervised learning and auto-adaptative architecture).

To unify the identification and the classification process, it has been chosen here to use a neural based classifier. As a basis, it has been chosen to use the cluster detection and labeling network (CDL) developed in 1998 by Eltoft and deFigueiredo [41]. For this classifier, the input vectors are compared with known "prototypes", then, in a second step, these prototypes are grouped into classes. Improvements have been brought by Lurette and Lecoeuche [42]. The new architecture is represented in Fig. 14.

The input layer consists of as many neurons as components of the input vectors. The hidden layer is totally connected to the input layer. Each neuron of the hidden layer represents a prototype of a class. The

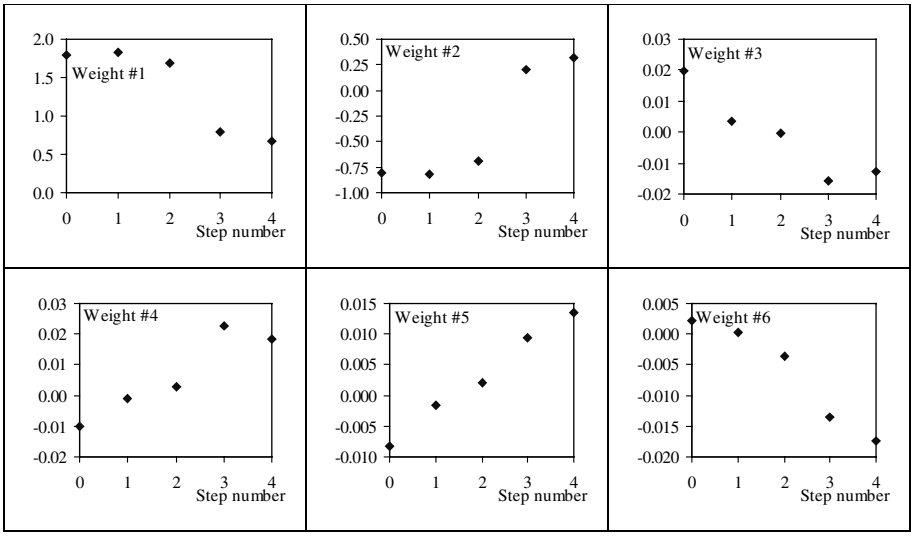

Fig. 12. Combined effects of viscosity and fouling on the weights (viscosity increase and fouling).

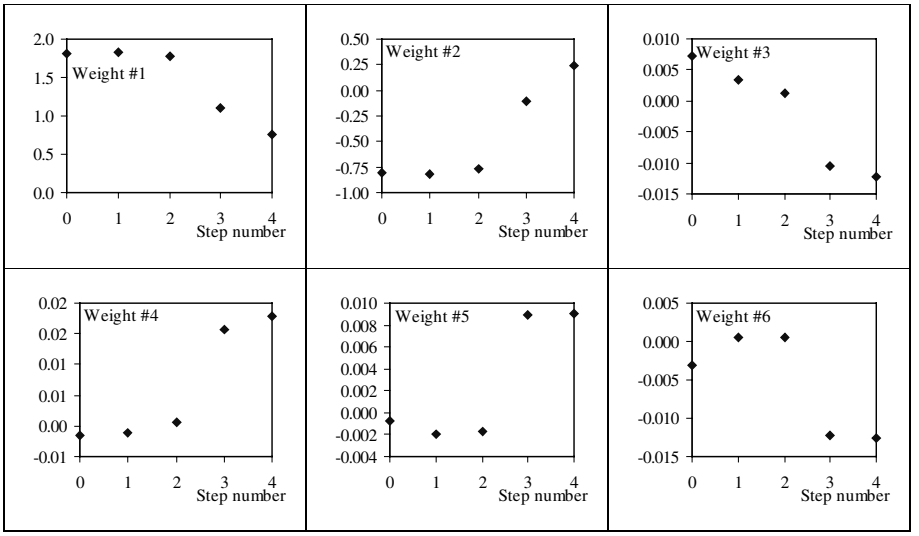

Fig. 13. Combined effects of viscosity and fouling on the weights (viscosity decrease and fouling).

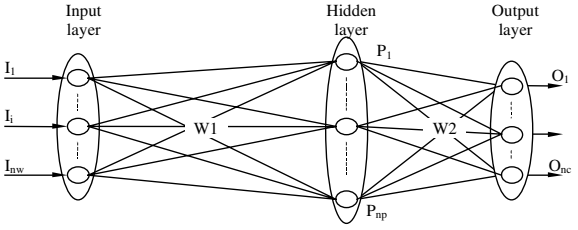

Fig. 14. New neural structure.

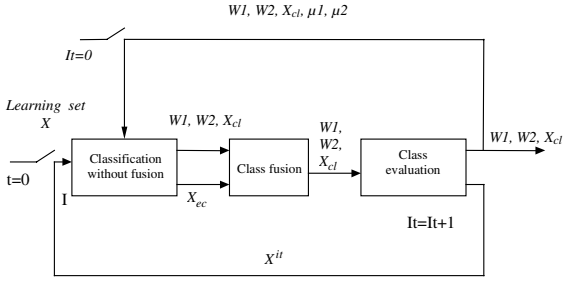

Fig. 15. CDL learning stages.

output layer consists of as many neurons as detected classes. The comparison between an input vector I and a known prototype P_j is made using the following activation function: $\mu(I,P_j)=\exp(-(1/2\sigma_j^2)D(I,P_j))$, where σ_j is linked to the sensibility of the classifier. The smaller σ_j, the higher the sensibility. The membership degree of an input vector to a class is defined as follows: $\psi(I,C_i)=\max(1,\sum_{P_j\in C_i}\mu(I,P_j))$. The learning and the adaptation of the network are made in three stages as shown in Fig. 15.

The first and main stage is called "classification without fusion". The particularity of this stage is to make possible the creation of a new prototype if the presented input vector is far from all the known prototypes. Similarly, a new class is created when a newly created prototype is very different from the already known prototypes. All the cases that have to be considered during this stage are summarized hereafter (Fig. 16):

The "class fusion" stage regroups classes that are close in the space representation. Each time an ambiguity is detected during the previous stage, the "class fusion" stage resolves it by merging the concerned classes. The ambiguous prototypes are associated to the new class. The output layer is modified by the elimination of the neurons that defined the ambiguous classes in order to keep a unique neuron (one neuron per ambiguity); this neuron being the result of the merged classes.

The "class evaluation" stage makes possible the characterization of the different classes in order to modify thresholds that are used in the computation. For example, a threshold could be used to eliminate classes containing too few assigned prototypes. These prototypes are marked as "unclassified", the similarity thresholds are modified in an iterative manner, and the "unclassified" examples are again presented to the neural network (for details cf. [42]).

6. Application to circulation heaters

To show the abilities of the second network, the following virtual sequence has been considered (Table 3); the step numbers refer to Figs. 10, 12, 13:

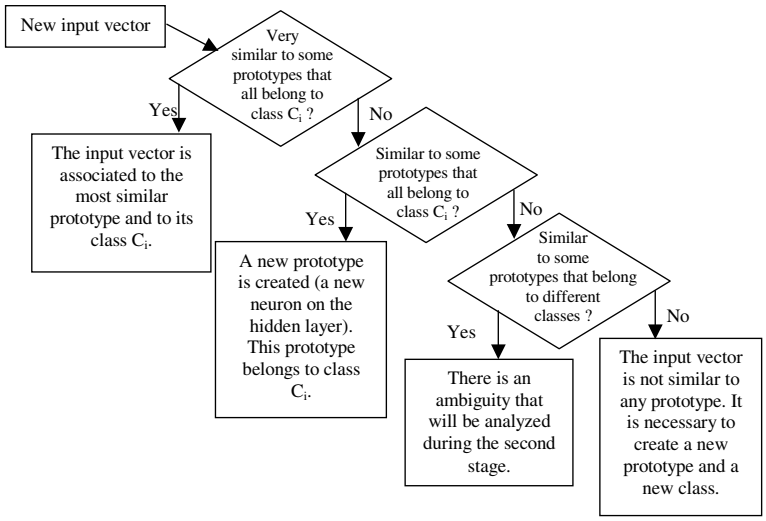

Fig. 16. Schematic of the "classification without fusion" stage.

Fig. 17 shows that when the classifier is not sensitive, it can detect the large drifts (drift #3 and #4), but not the small drifts.

When the sensitivity is increased, it is possible to detect the other drifts, but not to discriminate all of them; drifts #1 and #2 are considered as the first steps of drift #3 or #4 (Fig. 18).

It is possible to detect all the drifts by increasing again the sensitivity (Fig. 19).

In this last case, all the 16 combinations of connection weights, that correspond to the 16 drifts, have been detected. This proves that, even though the effects on the outlet fluid temperature are similar, fouling and viscosity modification have not the same effect on the connection weights. Hence, it can be concluded that the connection weights are trustful parameters to survey the current functioning of the heater.

Once the classes have been labeled, the classifier is frozen; i.e. neither new prototypes nor classes are created. So, the classifier is used as a normal classifier: when a new input vector is presented, it is associated with the nearest prototype and to its class. A quite large membership degree of the input vector to its associated class indicates that the present drift is actually similar to the previously detected drift. On the contrary, a quite small membership degree indicates that a new kind of drift occur. In practice, one would have to identify, on the ground, the new drift and should allow the classifier to

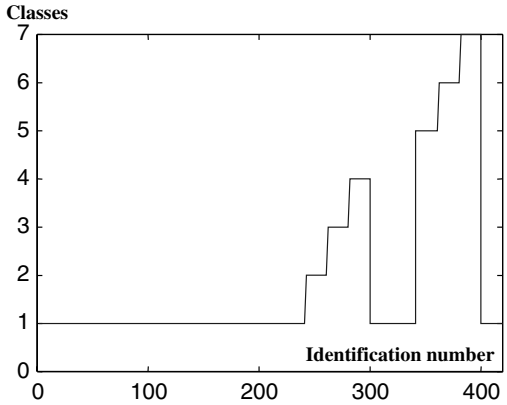

Fig. 17. Detection of large drifts.

Table 3
Definition of the considered drifts

	Clean heater	Fouling (drift #1)				Clean heater	Increasing viscosity (drift #2)			
		Step 1	Step 2	Step 3	Step 4		Step 1	Step 2	Step 3	Step 4
Id. #	1–20	21–40	41–60	61–80	81–100	101–120	121–140	141–160	161–180	181–200
		Fouling and increasing viscosity (drift #3)					Fouling and decreasing viscosity (drift #4)			
		Step 1	Step 2	Step 3	Step 4		Step 1	Step 2	Step 3	Step 4
Id. #	201–220	221–240	241–260	261–280	281–300	301–320	321–340	341–360	361–380	381–400

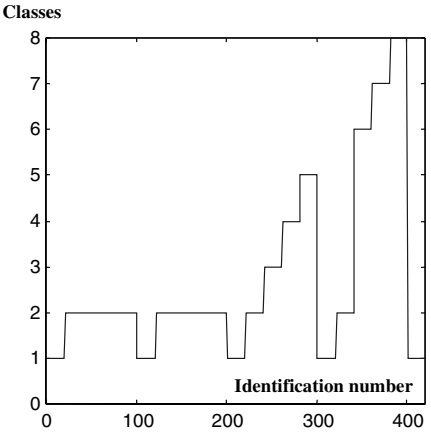

Fig. 18. Detection of all the drifts with lack of discrimination.

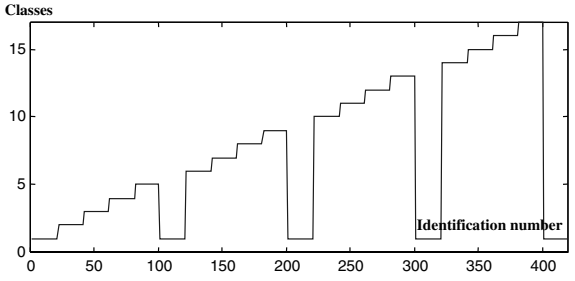

Fig. 19. Detection of all steps of all drifts.

evolve accordingly (to create a new prototype and a new class).

This shows that, during exploitation of the circulation heater, if the membership degree of an input vector to one of the classes that correspond to fouling is high, fouling is presently occurring in the circulation heater.

7. Conclusions

It has been shown that artificial neural networks can be successfully applied to monitor electrical circulation heaters and to discriminate fouling from viscosity modification. Two networks are used, the first one realizes the online identification of the system and the second one detects deviations and characterizes drifts.

It has been shown that identification of the system is only possible when enough information is contained in the sliding identification window.

A MISO model has been determined for the circulation heater. This model has been used to show that the connection weights of the model are trustful parameters for the determination of the functioning of the heater. It has been shown that the combinations of all the weights of the neural model depend on the origin of the drift (fouling, viscosity modification, ...). All these different combinations are detected by a neural network classifier (an improved CDL neural network) when the sensitivity of this network is well defined.

Ongoing studies address the experimental implementation of the system. Future studies will address heat exchangers that must be considered as MIMO (multiple inputs–mass flow rates and inlet temperatures—multiple outputs–outlet temperatures) systems.

References

[1] C. Renoult, J.P. Dechaume et al., Les techniques électriques pour les industries de la chimie, Les cahiers de l'ingénierie, Editions EDF 28 (1988) 4–8.
[2] P. Chretien, G. Deschamps, P. Le Peurian, Chauffage des fluides: l'échangeur électrique, Les cahiers de l'ingénierie, Editions EDF 37 (1990) 9–13.
[3] A. Bonet, Chauffage des fluides en circulation, une solution électrique à effet JOULE pour le chauffage des liquides et des gaz jusqu'à 1000 °C, Les cahiers de l'ingénierie, Editions EDF 43 (1992) 18–22.
[4] N. Lai, C. Nouar, R. Devienne, M. Lebouché, Transfert thermique pour des fluides pseudoplastiques dans des tubes à passage de courant de section annulaire, Congrès SFT 1997, Editions Elsevier, 1997, pp. 225–230.
[5] J.-F. Bourgeois, Régulation d'un réchauffeur électrique de fluides, Systèmes de régulation, MASSON, Paris, 1996, pp. 337–348.
[6] R.K. Shah, A.C. Mueller, Heat exchangers, fouling, in: W.M. Rohsenow, J.P. Hartnett, E.N. Ganic (Eds.), Handbook of heat transfer applications, second ed., McGraw-Hill, 1985, pp. 4-279–4-290.
[7] C.B. Panchal, E.-P. Huangfu, Effects of mitigating fouling on the energy efficiency of crude oil distillation, Heat Transfer Eng. 21 (3) (2000) 3–9.
[8] Y.I. Cho, B. Choi, Validation of an electronic anti-fouling technology in a single tube heat exchanger, Int. J. Heat Mass Transfer 42 (8) (1998) 1491–1499.
[9] Y.I. Cho, R. Liu, Control of fouling in a spirally-ribbed water chilled tube with electronic anti-fouling technology, Int. J. Heat Mass Transfer 42 (16) (1999) 3037–3046.
[10] W. Tae Kim, Y.I. Cho, C. Bai, Effect of electronic anti-fouling treatment on fouling mitigation with circulating cooling-tower water, Int. Commun. Heat Mass Transfer 28 (2001) 671–680.
[11] B. Thonon, S. Grandgeorge, C. Jallut, Effect of geometry and flow conditions on particulate fouling in plate heat exchangers, Heat Transfer Eng. 20 (3) (1999) 12–24.
[12] P. Terdtoon, C. Coykaen, S. Tungkum, K. Kraitong, Corrosion and fouling of tubes used in a thermosyphon economizer: a case study of paint protection, Appl. Thermal Eng. 20 (9) (2000) 791–801.
[13] I. Trentin, V. Romairone, G. Marcenaro, G. De Carolis, Quick test methods for marine antifouling paints, Progr. Organic Coat. 42 (2001) 15–19.
[14] M. Abu-Zaid, A fouling evaluation system for industrial heat transfer equipment subject to fouling, Int. Commun. Heat Mass Transfer 27 (6) (2000) 815–824.

[15] T.R. Bott, Biofouling control with ultrasound, Heat Transfer Eng. 21 (3) (2000) 43–49.
[16] S. Asomaning, A.P. Watkinson, Petroleum stability and heteroatom species effects in fouling of heta exchangers by asphaltenes, Heat Transfer Eng. 21 (3) (2000) 10–16.
[17] R. Sheikholeslami, Calcium sulfate fouling-precipitation or particulate: a proposed composite model, Heat Transfer Eng. 21 (3) (2000) 24–33.
[18] M.M. Prieto, J. Miranda, B. Sigales, Application of a stepwise method for analysing fouling in shell and tube exchangers, Heat Transfer Eng. 20 (4) (1999) 19–26.
[19] M. Prieto, J. Vallina, I. Suarez, Application of a design code for estimating fouling on-line in a power plant condenser refrigerated by seawater, Proceedings of The ASME-ZSITS International Thermal Science Seminar, Bled, Slovenia, June 11–14, on CD-ROM, 2000.
[20] J. Teeter, M.-Y. Chow, Application of functional link neural network to HVAC thermal dynamic system identification, IEEE Trans. Ind. Electron. 45 (1) (1998) 170–176.
[21] S.A. Kalogirou, Performance prediction of a solar water heater using artificial neural networks, Proceedings of the ISES 1999 Solar World Congress, Jerusalem, Israel, on CD-ROM, 1999.
[22] S.A. Kalogirou, Long-term performance predicting of forced circulation solar domestic water heating systems using artificial neural networks, Appl. Energy 66 (1) (2000) 63–74.
[23] S. Lalot, S. Lecoeuche, Identification of the time parameters of electrical heaters using artificial neural networks, Proceedings of the 34th ASME National Heat Transfer Conference, Paper NHTC2000-12153 on CD-ROM, 2000.
[24] J.M. Nougues, Y.G. Pan, E. Velo, L. Puigjaner, Identification of a pilot scale fluidised-bed coal gasification unit by using neural networks, Appl. Thermal Eng. 20 (15–16) (2000) 1561–1575.
[25] G. Diaz, M. Sen, K.T. Yang, R.L. McClain, Dynamic prediction and control of heat exchangers using artificial neuralnetworks, Int. J. Heat Mass Transfer 44 (9) (2001) 1671–1679.
[26] D.T. Pham, S.J. Oh, Identification of plant inverse dynamics using neural networks, Artificial Intelligence Eng. 13 (3) (1999) 309–320.
[27] J. Zhang, A.J. Morris, E.B. Martin, C. Kiparissides, Estimation of impurity and fouling in batch polymerization reactors through the application of neural networks, Comput. Chem. Eng. 23 (1999) 301–314.
[28] N. Delgrange, C. Cabassud, M. Cabassud, L. Durand-Bourlier, J.M. Lainé, Modelling of ultrafiltration fouling by neural network, Desalination 118 (1998) 213–227.
[29] S. Lecoeuche, C. Lurette, S. Lalot, Online identification and diagnostic method applied to thermal systems, Proceedings of the EANN 2000 conference, 17–19 July 2000, Kingston, Great Britain, 2000, pp. 155–162.
[30] C. Lurette, S. Lalot, S. Lecoeuche, Detection and diagnostic of drifts by unsupervised and autoadaptative neural network, Proceedings of the EANN 2001 Conference, 16–18 July 2001, Cagliari, Italy, 2001, pp. 239–246.
[31] J. Padet, Echangeurs thermiques, Masson, Paris, 1994.
[32] S. Lalot, Identification of solar collectors during service using artificial neural networks, Proceedings of the 2001 Solar World Congress, Adelaide (Australia), 25 November–2 December 2001, in press.
[33] K. Ljung, System identification—theory for the user, second ed., PTR Prentice Hall, Upper Saddle River, NJ, 1999.
[34] J. Sjöberg, Non-linear system identification with neural networks, Ph.D. thesis, Department of Electrical Engineering, Linköping University, Sweden, 1996.
[35] M. Norgaard, O. Ravn, N.K. Poulsen, L.K. Hansen, Neural networks for modeling and control of dynamic systems, Springer-Verlag, London, 2000.
[36] S. Lalot, S. Lecoeuche, Online identification of heat dissipaters using artificial neural networks, J. Mech. Eng. 47 (8) (2000) 411–416.
[37] S. Lalot, S. Lecoeuche, Online identification of circulation electrical heaters as MISO systems using artificial neural networks, Proceedings of the 35th ASME National Heat Transfer Conference, 10–12 June 2001, Anaheim (CA) Paper NHTC01-1811 on CD-ROM, 2001.
[38] S. Lalot, S. Lecoeuche, Identification en ligne et hors ligne de réchauffeurs électriques par réseaux de neurones, Trans. CSME 25 (3&4) (2001) 277–296.
[39] S. Lalot, W.J. Kaluba, J.-P. Marteel, Study of unstationary states of electrical heaters, Proceedings of the First International Conference of Heat Transfer with change of phase, Kielce, vol. 2, 1996, pp. 17–26.
[40] F.P. Incropera, D.P. de Witt, Fundamentals of heat and mass transfer, fourth ed., John Wiley, New York, 1996.
[41] T. Eltoft, R. deFigueiredo, A new neural network for cluster-detection-and-labeling, IEEE Trans. Neural Networks 9 (5) (1998) 1021–1035.
[42] C. Lurette, S. Lecoeuche, Improvement of cluster detection and labeling neural network by introducing elliptical basis function, Proceedings of the International Conference on Artificial Neural Networks, August 21–25, 2001 Vienna, Austria, pp. 196–202, 2001.